A new method to study shape recovery of red blood cells using multiple optical trapping

Bronkhorst, P.J.H.; Streekstra, G.J.; Grimbergen, J.A.; Brakenhoff, G.J.

DOI
10.1016/S0006-3495(95)80084-6

Publication date
1995

Published in
Biophysical Journal

A New Method to Study Shape Recovery of Red Blood Cells Using Multiple Optical Trapping

P. J. H. Bronkhorst, G. J. Streekstra, J. Grimbergen,* E. J. Nijhof,‡ J. J. Sixma, and G. J. Brakenhoff*
Department of Haematology, Universiteit Utrecht, *Department of Molecular Cytology, University of Amsterdam, Amsterdam, and ‡Helmholtz Instituut, Department of Physics of Man, Universiteit Utrecht, University Hospital, 3508 GA Utrecht, The Netherlands

ABSTRACT In this new method for studying the shape recovery of deformed red blood cells, three optical traps ("optical tweezers") induce a parachute-shaped red cell deformation, which is comparable to the deformation in small capillaries. The shape recovery is recorded, and a relaxation time is obtained for each individual red blood cell. The sensitivity of this technique for the detection of differences in relaxation times is demonstrated on subpopulations of density-separated red blood cells: "young" cells have shorter (162 ms) and "old" cells have longer (353 ms) relaxation times compared with the total population (271 ms). The relaxation time is remarkably shorter (114 ms) when the plasma surrounding the cells is replaced by a phosphate-buffered saline solution. The main advantages of this technique are the relatively short measuring and preparation time and the physiological type of deformation and shape recovery in which all relevant cell properties play a role. Therefore, especially when automated further, the technique may be a powerful tool for the study of (sub)populations of pathological red blood cells.

INTRODUCTION

An important factor regulating blood rheology is the deformability of the red blood cells (Weed, 1970; Chien, 1981; Chien, 1987). Red cell deformability is the combined result of several mechanical and geometrical properties of the red blood cells. Extrinsic factors such as internal viscosity and surface area-to-volume ratio of the cells, as well as membrane elasticity and viscosity, are determinants of the overall deformability of the red blood cells. A physiologically important aspect of red cell deformability is the ability of cells to change shape because it determines whether or not a cell can enter or pass through the small vessels of the microcirculation.

The technique that at present compares best with the physiological situation is red cell filtration (e.g. Teitel, 1977; Leblond and Coulombe, 1979; Koutsouris et al., 1988; Seiffge, 1988) where the ability of cells to enter and pass through narrow pores is measured. This technique is useful when looking at the overall filterability of the population. Information on individual cells in terms of deformability is difficult to obtain and interpret because every cell enters the pores differently, which means that the shape change differs for each cell.

Other methods for studying the ability of red blood cells to change shape record the shape recovery process (relaxation) of the cells after the removal of a defined and standardized deformation. The two techniques presently used for the measurement of shape recovery are the micropipette (Evans, 1989; Linderkamp and Meiselman, 1982; Nash and Meiselman, 1983) and the rheoscope (Sutera et al., 1985; Williamson et al., 1985). In the micropipette technique, the deformation is applied by partly aspirating part(s) of the cell into one or two pipettes. In rheoscopy, cells are ellipsoidally deformed in a linear shear flow. In both techniques the cells are observed microscopically. In these techniques, the shape recovery is determined mainly by membrane viscosity and elasticity (Linderkamp and Meiselman, 1982; Hochmuth et al., 1979; Fischer, 1980).

In the present work we present a new technique to study shape recovery of red blood cells. Red blood cells are deformed using multiple optical traps. The noncontact micromanipulator utilizing an optical trap, also called an "optical tweezer," was first demonstrated by Ashkin and Dziedzic (1987) and is an alternative to techniques using needles or micropipettes. It is becoming an important technique in the biomedical and biological sciences, and it has various applications (see overview given by Block, 1992). One such application is the measurement of the elastic properties of the isolated red blood cell skeleton (Svoboda et al., 1992).

Recently, Visscher et al. (1993) presented a method to create several optical traps. When these traps are positioned on different parts of a particle, it is possible to exert forces on the particle by moving the relative positions of the traps. We used three such traps to deform red blood cells into a parachute shape, which can be compared with the type of deformation found in small capillaries (Gaehtgens et al., 1980). When the traps are removed instantaneously, the cell relaxes back to its original shape. This shape recovery is recorded on video from which the relaxation time is obtained.

We carefully assessed the possible changes in the red blood cells induced by the optical trapping laser beam. On the basis of these experiments, we chose a measurement

Received for publication 28 December 1994 and in final form 27 July 1995.
Address reprint requests to Dr. Philippine J. H. Bronkhorst, Utrecht University Hospital, Department of Haematology, G.03.647, P. O. Box 85500, 3508 GA Utrecht, The Netherlands. Tel.: 31-3050-7769; Fax: 31-3051-1893; E-mail: jsixma@lab.azu.nl

0006-3495/95/11/1666/00 $2.00

protocol in which possible effects of the laser beam are negligible.

In order to show the usefulness and sensitivity of the technique, density-separated subpopulations are used. The measured relaxation times are compared with micropipette studies performed by Linderkamp and Meiselman (1982) and with rheoscopic experiments performed by Sutera et al. (1985). Because both groups performed their experiments in buffer and because we wished to interpret our results in plasma in comparison with theirs in buffer, we also did an experiment in buffer to see whether plasma and buffer give rise to differences in relaxation times.

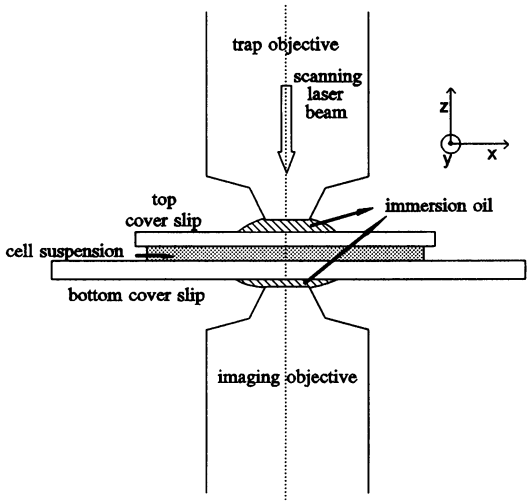

FIGURE 1 Schematic representation of the essential part of the experimental setup. The dilute suspension of red blood cells in plasma is located between two glass coverslips. The optical trapping laser beam is coupled into the trap objective (*top*), and the focal point is located between the two coverslips. The imaging is done by the bottom objective using phase contrast microscopy.

MEASUREMENT OF SHAPE RECOVERY OF RED BLOOD CELLS

Optical trapping principle

The focal spot of a sharply focused laser beam forms the tip of the "tweezer" and is called an optical trap. An object illuminated by such a focused laser beam experiences a scattering force based on radiation pressure that pushes it forward into the direction of the energy flux. In addition, a so-called gradient force is exerted on the particle. For particles with a diffractive index larger than the surrounding medium, the direction of this gradient force is toward regions with a higher intensity (Ashkin et al., 1986; Gordon, 1973). In regions close to the focal point of the laser beam, where the two forces have opposite signs and cancel each other, particles are trapped at a stationary three-dimensional position (Ashkin et al., 1986; Visscher and Brakenhoff, 1992a,b). By displacing the focal position of the laser beam in space, the trapped particle can be moved around. Particles with no spherical optical symmetry exhibit a self-orientation when they are in a trap. This phenomenon has also been observed for red blood cells (Ashkin, 1991).

Optical trapping instrumentation

The optical trapping instrumentation with multiple optical traps has been described in detail by Visscher et al. (1993). The most essential part of the experimental setup is depicted in Fig. 1. The condenser of an inverted microscope (Olympus IMT-2, Olympus Optical Co. Ltd., Tokyo, Japan) has been replaced by a dichroic mirror and a plan objective (100×, N.A. = 1.2 Nikon, Tokyo, Japan), through which an Nd:YAG laser beam (wavelength 1064 nm; Spectron Laser Systems, Warwickshire, UK) is applied. Multiple traps are created by scanning one single beam trap along a variable number of positions in the horizontal plane, which is controlled interactively by a UNIX workstation (Hewlett Packard model 725/50) coupled to a VME instrumentation bus. This instrumentation bus controls the positions of two perpendicular scanning mirrors, which determine the position of the laser beam in the horizontal plane. Between the desired trap positions, the laser beam is blocked using an Acoustic-Optic Modulator (AOM, IntraAction Corp. Bellwood, IL). The red blood cells are moved relative to the traps by moving the microscope stage in the horizontal plane. Microscopic imaging is done with a 100× phase contrast, oil immersion objective (N.A. = 1.3 Leitz, Wetzar, Germany) using a videocamera (25 Hz CCD camera FA 85 I, Grundig Electronic, Fürth, Germany). A magnification lens of 6.7× and an infrared blocking filter are placed in the light path, the latter to prevent overexposure of the camera by the infrared laser light used for trapping.

The suspension of red blood cells is located between two glass coverslips (20–30 μm in between) between the two objectives. The sample is sealed by nail polish to avoid convection during the experiment.

Measuring principle

Because a red blood cell is relatively large compared with the dimension of the beam waist of the optical trap, it can be trapped at several locations simultaneously. Red blood cells always orient parallel to the direction of the laser beam in a single optical trap as a result of the direction of the laser beam waist in combination with the nonspherical symmetry of the cells. We use three traps at standardized locations and two different configurations. First, a cell is lifted from the bottom with the traps in the configuration depicted in Fig. 2 *A* and is in the focus of the imaging objective when stable in the trap. During the lifting process, the cell orients vertically along the optical axis. Then, the middle spot is moved to the left at a standardized low speed, which deforms the cell into a parachute shape (see Fig. 2 *B*). When the configuration of Fig. 2 *B* is reached, the laser is turned

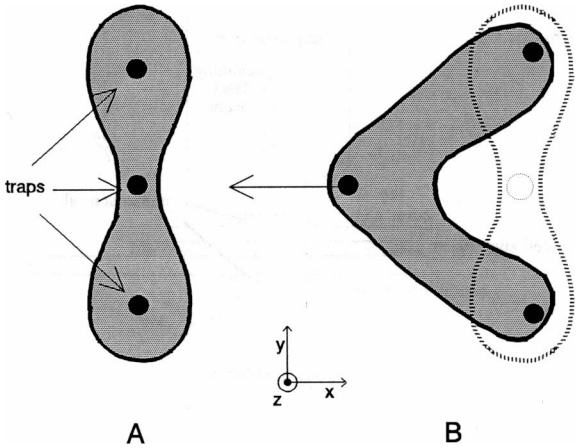

FIGURE 2 Three traps are used to deform the red blood cell, as is viewed along the optical axis (*z-axis*). (*A*) Start configuration: the red blood cell orients vertically in the traps and is in focus of the imaging objective when the cell is stable in the trap. (*B*) The cell is deformed into a parachute shape by moving the middle spot to the left at a standardized low speed.

off and the cell relaxes to its original shape while remaining vertically oriented. This shape recovery is recorded on video.

The manipulation and location of the spots is standardized and is computer controlled. Because dilatation of the red cell is impossible without damaging the membrane, care was taken in choosing the standard locations of the spots. This means in practice that we chose the outer spot locations not too far apart so that all individual cells within a population could be deformed sufficiently.

The frequency at which the laser beam is scanned along the three trap positions is 50 Hz, which was found to be appropriate for the red blood cells. In all experiments, the power of the optical trapping laser beam, as measured at the entrance of the trapping objective, was ~220 mW. With this power, the deforming force was just sufficient to deform all individual cells within a population. An example of a relaxation is shown in Fig. 3.

The preparation time can be very short as the only preparation needed before an experiment is to seal the sample between the two coverslips. The time per measurement can be short too: the microscope stage is moved until a new cell is found (which can be done very quickly). The traps are then turned on, and the cell is lifted from the bottom. The deformation and relaxation process can be performed within a few seconds. In this way, 50 or more cells per hour can be measured.

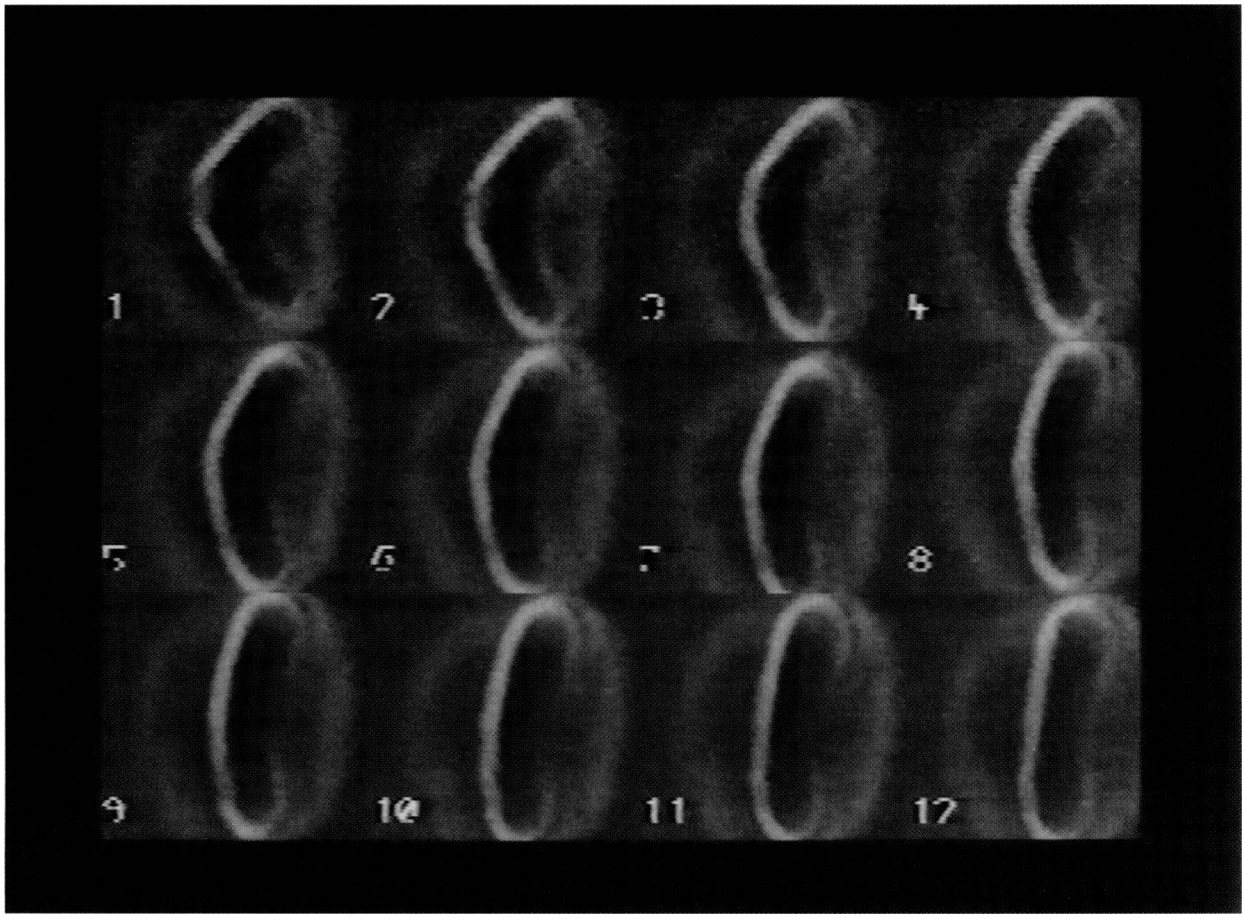

FIGURE 3 An example of a relaxation of a red blood cell. The time between frames is 40 ms.

Off-line analysis of the deformation

The analysis is done from videotape using a video recorder with a frame by frame viewing option (25 Hz refresh rate). The frames containing the relaxing cell are digitized using a frame grabber, resulting in a combined image such as Fig. 3. Subsequently, the angle α between the two sides of the cell is measured per frame. For this purpose, software was developed using line-shaped cursors that can be moved and rotated within the image. This enables us to measure the angle accurately. The sides are usually the most visible part of the cells, and the angle changes over a large range during the relaxation. Fig. 4 shows an example of a measurement of the angle α versus time.

$$\alpha(t) = (180 - \alpha(0))(1 - \exp(-t/\tau)) + \alpha(0) \qquad (1)$$

An exponential curve (1) is fitted through the data points from which the relaxation time $t_{1/2} = \tau \times \ln(2)$ and a fit error are obtained.

During the relaxation the dimple returns, making it more difficult to measure the angle accurately. Because this usually results in a systematic error, we use only the initial relaxation by omitting from the fit procedure the points with angles larger than $\approx 150°$. In the fit procedure the data are linearized first and $\alpha(0)$ and τ are calculated using linear regression.

RED BLOOD CELL PREPARATIONS

Blood was drawn from a healthy donor and anticoagulated with citrate (1:10 v/v 110 mM trisodium citrate). Plasma from the same donor, obtained by centrifuging at 1000 × g for 15 min, was filtered using a 0.2 μm Minisart NML SM 16534 K (Sartorius Ltd., Epsom, UK) to remove small particles, especially platelets, which can also be caught in the traps and may disturb the measurement.

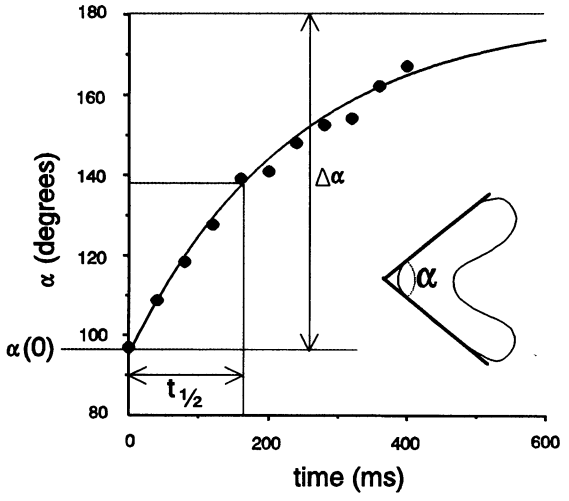

FIGURE 4 The deformation angle α versus time together with a fitted exponential curve. The relaxation time $t_{½}$ is defined as the time needed to reach the angle $\alpha(0) + ½\Delta\alpha$ degrees.

The measurements were carried out in native plasma or in a buffer solution at a hematocrit of 0.4%. The buffer that was used contained 90% phosphate-buffered saline (10 mM sodium phosphate and 145 mM NaCl, pH = 7.4) containing 1 g/l bovine serum albumin (Sigma, St. Louis, MO) and 10% native plasma; 0.4 wt % polyvinylpyrrolidone (P.V.P. 360000, Sigma) was added to increase the medium viscosity. The experiments were started directly after the cells were added to the medium. The density separation of red blood cells was performed using the "percoll" method described by Rennie et al. (1979). We used percoll concentrations of 80%, 72%, 65%, 59%, and 40%. A suspension of washed packed cells was added on top of this stack, and the whole tube was centrifuged for 15 min at 1030 × g at room temperature. In the experiment shown in this paper, the 40% and 59% fractions contained hardly any cells. Therefore, the 65% fraction was used as the top fraction because it contained the bulk of the least dense cells of the population. The bulk of the most dense cells was on top of the boundary layer of the 72% and 80% fraction, which was therefore chosen as the bottom fraction. The fractions were washed twice in phosphate-buffered saline solution to remove the percoll, and the cells were suspended in the native plasma. The mean cell volumes were measured on a Sysmex counter (TOA Medical Electronics, Kobe, Japan).

EXPERIMENTS

Control experiments

To ensure that the measurement procedure, in particular the exposure of the cells to the optical trapping laser beam, did not harm the cells or affect the measured $t_{½}$, several control experiments were performed. First we measured how long cells can be kept in the traps before they are damaged. We found that the cells can be kept in the traps for at least 1 min before morphological changes occur and the cell cannot be deformed anymore. The cells lose their biconcave shape and become spherical, and their membrane loses its smooth outlook. These morphological changes are likely to be caused by excessive heating by the laser light.

Secondly we checked to determine whether a measurement affects the measured $t_{½}$ by repeated deformation and relaxation of the same cell, both in plasma and in buffer. The cells were kept in the traps for as short a period of time as possible (a few seconds). After 15 to 20 relaxations, the cells showed the drastic morphological changes mentioned before. The total time in the trap is then comparable to the time a cell can be trapped continuously before the morphological changes occur. There was no change in morphology up to five to eight times, but after these five to eight times the dimple often did not return at the left side. However, this small morphologic change did not affect the measured $t_{½}$ as there was no correlation between the relaxation time and the relaxation number. Fig. 5 shows the results for one cell.

With these results in mind, we standardized the measurement in order to reduce the time needed for one relaxation

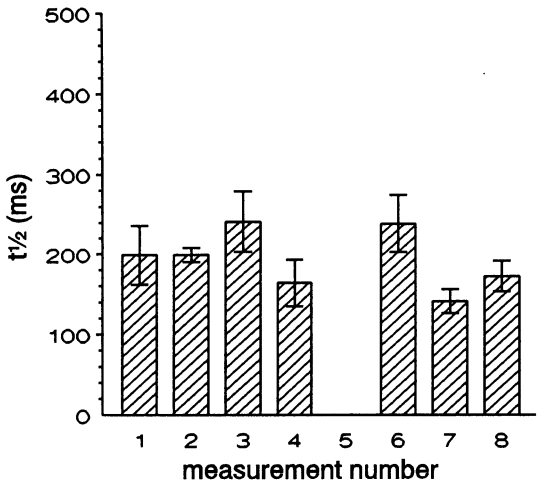

FIGURE 5 An example of a repeated relaxation (1–8) of one cell showing no significant change in the $t_{1/2}$. Relaxation 5 was omitted because the cell was not properly in focus during the shape recovery and therefore could not be analyzed. The error bars represent the fit error.

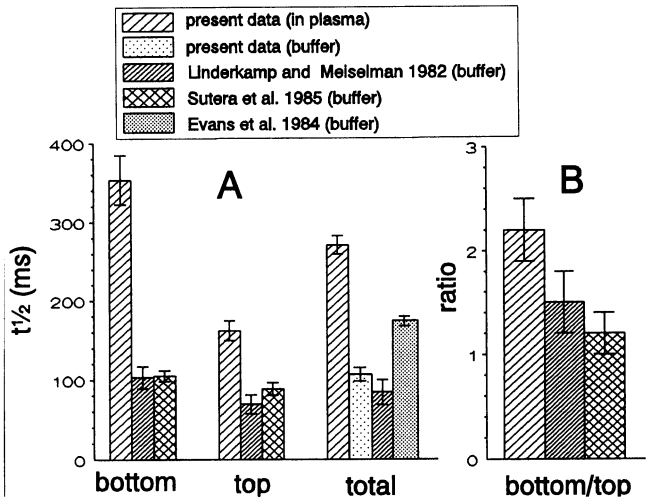

FIGURE 6 The present data and the results of Linderkamp and Meiselman (1982, micropipette) and Sutera et al. (1985, rheoscope), and the bending relaxation study of Evans et al. (1984, micropipette). (*A*) Absolute values of the relaxation times of the various fractions. The $t_{1/2}$ in buffer compares with the other data, and the $t_{1/2}$ in plasma is strongly increased when compared with buffer. The present data are the weighted mean of the relaxation times ($t_{1/2}$) of density-separated fractions in plasma and of cells in buffer. (Bottom fraction: $n = 39$, mean cell volume (MCV) = 87 fl; top fraction: $n = 34$, MCV = 100 fl; the total population: $n = 34$, MCV = 91 fl; total population in buffer: $n = 22$.) The error bars represent the standard deviations. (*B*) Relative differences between the density-separated fractions: the ratio of the relaxation times of the bottom fraction and the top fraction. Our technique shows larger relative differences in $t_{1/2}$ between old and young cells when compared with the other techniques.

as much as possible. A cell was never deformed more than once, and the time that the cell was kept in the trap was minimized. Usually, a cell was in the trap for 2–5 s before the deformation, and if it was in for more than 10 s we excluded it from the measurements.

Density-separated red blood cells

It has been demonstrated (e.g., Linderkamp and Meiselman, 1982; Sutera et al. 1985) that red cell deformability is different between the most dense ("old") and the least dense ("young") cells of a normal population. With these results in mind, we chose to demonstrate the sensitivity of the technique on density-separated subpopulations.

As expected we found differences in relaxation times between the density-separated fractions: cells of the bottom fraction (dense cells) have longer relaxation times (353 ms) and cells of the top fraction (least dense cells) have shorter relaxation times (162 ms) than those of the total fraction (271 ms), as is depicted in Fig. 6.

When the results per fraction are depicted in a frequency distribution (Fig. 7), we see that there are enormous variations in the relaxation time. Notably the bottom fraction contains extremely slow cells (7 of 39 cells have relaxation times longer than 675 ms).

Plasma versus buffer

Because plasma is more physiological than buffer and our setup allows us to use plasma, plasma was chosen as suspending medium. However, buffer solutions are usually used in shape recovery studies (Linderkamp and Meiselman, 1982; Sutera et al., 1985). Therefore we also did an experiment in buffer with the same donor to investigate whether or not there is a difference in the shape recovery between plasma and buffer as suspending medium.

We found that in such buffer experiments, the presence of relatively large areas of glass near the cells in combination with the absence of plasma proteins caused experimental problems. (1) The cells attached to the bottom glass coverslip, (2) echinocytes were formed, and (3) more vibration and higher sedimentation rates were found in the buffer because of the lower medium viscosity. To prevent the problem of vibration and higher sedimentation rates, a small amount of a high molecular weight polymer (polyvinylpyrrolidone) was added, which increased the medium viscosity to 2 mPas (plasma was 1.5 mPas). To prevent the attachment of cells to the bottom glass coverslip and the formation of echinocytes as much as possible, 1 g/l bovine serum albumin and 10% native plasma were added to the phosphate-buffered saline solution. The results of the relaxation times in plasma compared with buffer (both for the total population) are also depicted in Fig. 6. The $t_{1/2}$ is strongly decreased in buffer with the plasma-to-buffer ratio of 2.4. In buffer we did see some echinocytes (5–10%), and part of the remaining population looked somewhat crenated as well. Because echinocytes and crenated cells were excluded from the measurements, cell selection of the less fragile (younger?) fraction of cells occurs. However, this selection can only partly explain the differences between plasma and

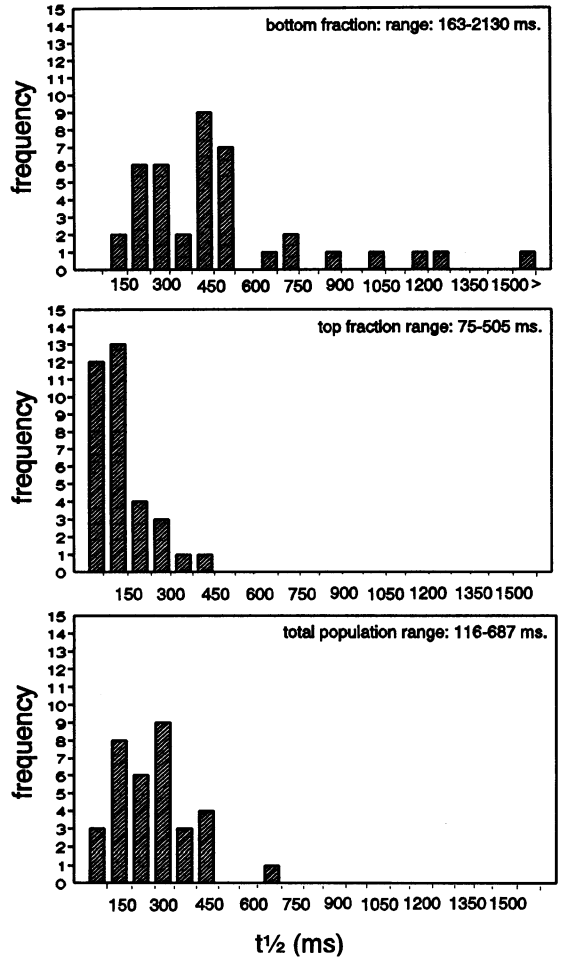

FIGURE 7 Frequency distributions of the $t_{1/2}$ of the cells in the bottom and top fractions and of the total population in plasma. Interval width is 75 ms. The bottom fraction contains a large number of cells with extremely high $t_{1/2}$.

buffer because the relaxation times in buffer are even shorter than those of the young fraction of cells in plasma.

DISCUSSION

The method we presented has proven to be useful to study relaxation times of red blood cells. Our more complex type of shape recovery, in which a deformation similar to the deformation found in small capillaries is used and in which all relevant cell properties play a role in determining the relaxation time, may be a good model for shape changes in vivo. Therefore, we think that the technique, especially when automated, may be useful for physiologically relevant studies.

All relaxation times as measured using optical trapping are of the same order of magnitude as compared to other techniques (Linderkamp and Meiselman, 1982; Sutera et al., 1985; Evans et al., 1984). However, as could be expected, our results in isotonic buffer compare best with the other shape-recovery studies, which were also performed in buffer.

Shape-recovery mechanism

When we regard our type of deformation and shape recovery and compare it with the type of deformation in the micropipette technique, we think that elastic and viscous components both play a role in our type of shape recovery. In the micropipette technique, the time constants for shear elastic shape recovery (τ_s) and for unfolding (τ_b) have been formulated by Evans (1989):

$$\tau_s \approx \frac{\eta_m + \eta_f\delta}{\mu} \approx \frac{\eta_m}{\mu} \qquad \tau_b \approx \left(\nu + \frac{\eta_f\delta}{\Delta C_m^2}\right)\Big/ B \qquad (2)$$

where η_m is the membrane viscosity, η_f is the effective viscosity due to the viscous dissipation of the internal and external fluid phases, and ν represents the viscous dissipation in bending of the membrane. ΔC_m is the curvature of the fold, and δ is the characteristic dimension of the cell. The elastic components are represented by μ and B, which are the shear modulus and bending modulus, respectively.

Our shape recovery is probably a combination of shear elastic shape recovery and unfolding. Therefore we assume in a first approximation that the time constant of our shape recovery can be described by a combination of τ_s and τ_b. This assumption is confirmed by our results because the relaxation times in our system are longer when compared with the micropipette (Linderkamp and Meiselman et al., 1982) and rheoscope (Sutera et al., 1985) elastic shape-recovery studies, but shorter when compared with the unfolding relaxation time (Evans et al., 1984).

Cell aging

During aging, both the membrane shear elasticity and the membrane viscosity increase by 20% and 80%, respectively (Linderkamp and Meiselman, 1982). Furthermore, the internal viscosity can increase up to 400% (Williams and Morris, 1980). The increase in internal viscosity is mainly caused by volume loss and to a lesser extent by glycosylation of hemoglobin (Sutera et al., 1985). Membrane viscosity increases due to glycosylation of membrane proteins and binding of hemoglobin to the cytoskeleton (Nash and Meiselman, 1983). Therefore the main change in the mechanical properties of old cells compared with young cells is an increase in η_f and η_m. This increase in η_f and η_m explains why old cells have longer relaxation times than young cells do (see Eq. 2).

The sensitivity to age-related differences seems to be higher in our technique than in the micropipette technique (Fig. 6 *B*). We find larger differences in relaxation times between old and young cells than those found by Linderkamp and Meiselman (1982). This is understandable because in our shape recovery, apart from the shear elastic recovery (τ_s), unfolding shape recovery (τ_b) also plays a role, whereas in the experiments by Linderkamp and Meiselman (1982) only τ_s determines the shape recovery. The involvement of τ_b in the shape recovery dramatically

increases the sensitivity to the internal viscosity (η_f, see Eq. 2). This dependence on internal viscosity may explain the presence of the subpopulation of cells in the bottom fraction with extremely long relaxation times (Fig. 7). This subpopulation probably correlates with the extremely high viscosities in the densest cells (Williams and Morris, 1980). However, although we found no evidence for it, the large range of relaxation times in the bottom fraction may be caused partly by a larger effect of heat-mediated damage to the densest cells.

Plasma versus buffer

Our findings in buffer compared with plasma are remarkable: a strongly increased relaxation time in plasma when compared with buffer. We do not expect that volume changes have occurred because the buffer used was isotonic. Furthermore, this difference cannot be caused by the different medium viscosity because then we would have expected a longer relaxation time in buffer because of the higher medium viscosity compared with plasma. Therefore, changes in membrane properties are likely to be responsible for the effect: an increased membrane bending (B) or shear elasticity (μ) or a decreased membrane viscosity (η_m) in buffer. The absence of plasma proteins and/or the different ion composition in buffer apparently lead to a change in the membrane mechanical properties. The fact that some echinocytes were present and that some of the other cells looked somewhat crenated supports this assumption. Even though these crenated cells were not used in the analysis, the remaining part of the "normal" cells may have had (although not visible) changed membrane properties as well.

Changes in membrane properties must have an origin in molecular changes in the cytoskeleton, in the bilayer, or in the association between the cytoskeleton and the bilayer. The cytoskeleton is the principle source of the shear elasticity as it is the only in-plane solid element in the membrane (Steck, 1989). The ion composition is known to affect the elasticity of the skeleton (Svoboda et al., 1992). The different ion composition in buffer may also change the internal ion composition and therefore the skeleton, e.g., via the Na^+K^+ pump and ATP depletion (Palek and Liu, 1979). In contrast to shear elasticity, the bending elasticity is mainly determined by the bilayer (Steck, 1989; Svoboda et al., 1992). The bilayer coupling effect probably changes bending elasticity as it is also responsible for the echinocyte formation and crenation (Steck, 1989). An increase in the shear elastic modulus or bending elastic modulus both result in a decreased relaxation time (see Eq. 2).

Another possible explanation lies in the absence of plasma proteins. Plasma proteins can adhere to the outer membrane surface, which may affect the membrane viscosity or change the electrostatic equilibrium in the vicinity of the cell membrane.

At this point it cannot be said which mechanisms are responsible for the difference between plasma and buffer. Additional research needs to be carried out in the near future in order to find the cause of this effect, by systematically changing the composition of the medium surrounding the cells.

CONCLUSIONS

Multiple optical trapping of red blood cells, as presented here, is found to be a potentially powerful new technique to study shape recovery of red blood cells. From a physiological point of view, our technique has the advantage that the measurements can easily be done in plasma, and the induced deformation is comparable to the type of deformation observed in capillaries. From a methodological point of view, optical trapping has the advantage of being able to measure large numbers of individual cells in a relatively short period of time. In the near future, the total measurement time will be reduced even more by increased automatization of the image analysis procedure.

By itself, the measured relaxation time does not provide direct quantitative information about individual mechanical cell properties. To obtain these cell properties, a rheological model describing the shape recovery is essential. Application of the models for elastic shape recovery and unfolding developed by Evans (1989) proved to be useful as a first step in modeling the complex shape recovery in our system. In the future, more adequate modeling will be carried out in order to quantitatively interpret the results in terms of cellular properties.

The authors wish to thank S. S. Adriaansen-Slot for helping with the density separation procedure and E. J. Gijsbers for developing the optical trap manipulation software. This research was supported by The Netherlands Heart Foundation (Grant 91.134) and by Stichting Technische Welenschappen (Grant ANS 33.2941).

REFERENCES

Ashkin, A. 1991. The study of cells by optical trapping and manipulation of living cells using infrared laser beams. *ASGSB Bull.* 4:133–146.

Ashkin, A., J. M. Dziedzic, J. E. Bjorkholm, and S. Chu. 1986. Observation of a single-beam gradient force optical trap for dielectric particles. *Optic Lett.* 11:288–290.

Ashkin, A., and J. M. Dziedzic. 1987. Optical trapping and manipulation of viruses and bacteria. *Science.* 235:1517–1520.

Block, S. M. 1992. Making light work with optical tweezers. *Nature.* 360:493–495.

Chien, S. 1981. Haemorheology in disease: pathophysiological significance and therapeutic implications. *Clin. Hemorheol.* 1:419–442.

Chien, S. 1987. Red cell deformability and its relevance to blood flow. *Annu. Rev. Physiol.* 49:177–192.

Clark, M. R., N. Mohandas, D. Feo, M. S. Jacobs, and S. B. Shohet. 1981. Separate mechanisms of deformability loss in ATP-depleted and Ca-loaded erythrocytes. *J. Clin. Invest.* 67:531–539.

Evans, E. A. 1989. Structure and deformation properties of red blood cells: concepts and quantitative methods. *Methods Enzymol.* 173:3–35.

Evans, E. A., N. Mohandas, and A. Leung. 1984. Static and dynamic rigidities of normal and sickle erythrocytes. Major influence of cell hemoglobin concentration. *J. Clin. Invest.* 73:477–488.

Fischer, T. 1980. On the energy dissipation in a tank-treading human red blood cell. *Biophys. J.* 32:863–868.

Gaehtgens, P., C. Dührssen, and K. H. Albrecht. 1980. Motion, deformation, and interaction of blood cells and plasma during flow through narrow capillary tubes. *Blood Cells*. 6:799–812.

Gordon, J. P. 1973. Radiation forces and momenta in dielectric media. *Phys. Rev.* 8:14–21.

Hochmuth, R. M., P. R. Worthy, and E. A. Evans. 1979. Red blood cell extensional recovery and the determination of membrane viscosity. *Biophys. J.* 26:101–114.

Koutsouris, D., R. Guillet, J. C. Lelievre, M. T. Guillemin, P. Bertholom, Y. Beuzard., and M. Boynard. 1988. Determination of erythrocyte transit times through micropores. I. Basic operational principles. *Biorheology*. 25:763–772.

Leblond, P. F., and L. Coulombe. 1979. The measurement of erythrocyte deformability using micropore membranes. A sensitive technique with clinical applications. *J. Lab. Clin. Med.* 94:133–143.

Linderkamp, O., and H. J. Meiselman. 1982. Geometric, osmotic, and membrane mechanical properties of density-separated human red cells. *Blood*. 59:1121–1127.

Nash, G. B., and H. J. Meiselman. 1983. Red cell and ghost viscoelasticity. Effects of hemoglobin concentration and in vivo aging. *Biophys. J.* 43:63–73.

Palek, J., and S.-C. Liu. 1979. Dependence of spectrin organization in red blood cell membranes on cell metabolism: implications for control of red cell shape, deformability, and surface area. *Semin. Hematol.* 16:75–93.

Rennie, C. M., S. Thompson, A. C. Parker, and A. Maddy. 1979. Human erythrocytes fractionation in "Percoll" density gradients. *Clin. Chim. Acta*. 98:119–125.

Seiffge, D. 1988. Analysis of the passage of single blood cells in a single pore filtration system. *Clin. Hemorheol.* 8:445–451.

Steck, T. L. 1989. Red cell shape. *In* Cell shape: Determinants, Regulation and Regulatory Role. W. Stein and F. Donner, editors. Academic Press, New York. 205–246.

Sutera, S. P., R. A. Gardner, C. W. Boylan, G. L. Carroll, K. C. Chang, J. S. Marvel, C. Kilo, B. Gonen, and J. R. Williamson. 1985. Age related changes in deformability of human erythrocytes. *Blood*. 65: 275–282.

Svoboda, K., C. F. Schmidt, D. Branton, and S. M. Block. 1992. Conformation and elasticity of the isolated red blood cell membrane skeleton. *Biophys. J.* 63:784–793.

Teitel, P. 1977. Basic principles of the "Filterability Test" (FT) and analysis of erythrocyte flow behavior. *Blood Cells (Berl)*. 3:55–70.

Visscher, K., and G. J. Brakenhoff. 1992a. Theoretical study of optically induced force on spherical particles in a single beam trap I: Rayleigh scatterers. *Optik*. 89:174–180.

Visscher, K., and G. J. Brakenhoff. 1992b. Theoretical study of optically induced force on spherical particles in a single beam trap II: Mie scatterers. *Optik*. 90:57–60.

Visscher, K., G. J. Brakenhoff, and J. J. Krol. 1993. Micromanipulation by "multiple" optical traps created by a single fast scanning trap integrated with the bilateral confocal scanning laser microscope. *Cytometry*. 14: 105–114.

Weed, R. I. 1970. The importance of erythrocyte deformability. *Am. J. Med.* 49:147–150.

Williams, A. R., and D. R. Morris. 1980. The internal viscosity of the human erythrocyte may determine its life span in vivo. *Scand. J. Haematol.* 24:57–62.

Williamson, J. R., R. A. Gardner, C. W. Boylan, G. L. Carroll, K. Chang, J. S. Marvel, B. Gonen, C. Kilo, R. Tran-Son-Tay, and S. P. Sutera. 1985. Microrheologic investigation of erythrocyte deformability in diabetes mellitus. *Blood*. 65:283–288.